



## A Top-Down Route for Preparation of Ultrathin Zinc Oxide Nanowires

Shiyao Zhu<sup>1,†</sup>, Ming Yang<sup>2,†</sup>, Ziwei Liu<sup>1</sup>, Shihui Jiao<sup>1</sup>,  
Guangsheng Pang<sup>1,\*</sup>, and Shouhua Feng<sup>1</sup>

<sup>1</sup>State Key Laboratory of Inorganic Synthesis and Preparative Chemistry, Jilin University,  
Changchun 130012, P. R. China

<sup>2</sup>Key Laboratory of Micro-Systems and Micro-Structures Manufacturing, Ministry of Education,  
Micro/Nano Technology Research Center, Harbin Institute of Technology, Harbin 150080, P. R. China

Zinc oxide nanowires have been successfully obtained through the splitting of layered basic zinc acetates. The layered basic zinc acetates nanobelts served as intermediates are prepared by adding water into zinc oxide ethanol colloids. Zinc oxide nanowires have uniform diameters of about 3–5 nm and lengths of several hundred nanometers. The formation mechanism of zinc oxide nanowires is proposed. The mechanism is that zinc oxide nanowires are generated by the splitting of the layered compound. From this mechanism, we find that the structure characteristic of layered basic zinc acetates is essential for the formation of ZnO nanowires. We also discuss the relationship between the morphology of products obtained after incubating and incubating time. The products are characterized by X-ray powder diffraction, transmission electron microscopy, scanning transmission electron microscopy and infrared spectrum.

**Keywords:** Layered, Top-Down, Splitting, ZnO Nanowires.

### 1. INTRODUCTION

One-dimensional (1-D) nanomaterials have been extensively studied due to their unique applications in mesoscopic physics and fabrication of nanodevices.<sup>1,2</sup> A variety of effective methods have been applied in the synthesis of 1-D nanostructures, such as vapor–liquid–solid growth process,<sup>3,4</sup> chemical vapor deposition,<sup>5</sup> thermal evaporation,<sup>6,7</sup> reverse micelles,<sup>8</sup> template-confined method,<sup>9,10</sup> and self-assembly of nanoparticles.<sup>11,12</sup> Generally, the above mentioned methods are so called “bottom-up” method. Another strategy to obtain nanomaterials is so called “top-down” method which involves extraction of a nanowire from a bulk sample by thinning through processes such as electron-beam, optical-beam, ion-beam and scanning-probe lithography.<sup>13–15</sup>

ZnO nanowires (NWs) are important wide band gap (3.37 eV at 298 K) semiconductor with a large exciton binding energy (60 meV) and have received extensive interest<sup>16,17</sup> for application in electronic and optoelectronic devices, such as solar cells,<sup>18,19</sup> light emitting diodes,<sup>20</sup>

and field-effect transistors.<sup>21</sup> It is well-known that the quantum confinement effect has become evidence for nanostructures with sizes comparable to the exciton Bohr radius.<sup>22</sup> In general, ultrathin ZnO NWs with diameters below 10 nm are expected to display novel and unique physical and chemical properties due to quantum confinement.<sup>23,24</sup> ZnO NWs can be considered as 1-D channel under emission and transport of electrons, holes, and photons. The special geometry structure can lead to strong confinement effect on the carriers and photons, which can result in various novel electrical and optical properties for device applications such as short wavelength LEDs and lasers of nanometer size.<sup>25,26</sup> Furthermore, Lee et al.<sup>27</sup> found that, with the decrease of the diameter of the NWs, Young’s modulus, stress–strain behavior, and yielding stress all increased. It indicated that ultrathin ZnO NWs possessed very high malleability. The compounds with layered structures may be served as intermediates for the formation of NWs. Li’s group had endeavored to explore new types of inorganic NWs from layered precursors based on a rolling mechanism.<sup>28–30</sup> ZnO NWs were prepared from a layered precursor by a solution route in the presence of poly(vinyl pyrrolidone).<sup>31</sup> Here, we

\*Author to whom correspondence should be addressed.

†These two authors contributed equally to this work.

reported a novel top-down method to prepare 1-D ZnO NWs, and the formation process could be described as the splitting of layered basic zinc acetates (LBZA).

## 2. EXPERIMENTAL DETAILS

### 2.1. Synthesis of LBZA NBs

Zinc acetate dehydrate (0.01 mol) was dissolved in ethanol (100 mL) and heated at reflux for 2 h at 80 °C. The solution was then cooled to room temperature and KOH (0.015 mol) ethanol solution (100 mL) was added. The above solution was then placed in an ultrasonic bath to accelerate the reaction for 1 h, so the transparent ZnO colloids were obtained. Then, 10 mL distilled water was dropwise added in 20 mL ZnO ethanol colloids. After 30 min, the white precipitates were collected by centrifugation.

### 2.2. Synthesis of ZnO NWs

The as-prepared NBs were directly dispersed into 10 mL distilled water and then kept for 2 days.

### 2.3. Characterizations

Powder X-ray diffraction (XRD) analysis was performed with a Rigaku D/MAX 2550 V/PC diffractometer with a Cu K $\alpha$  radiation ( $\lambda = 1.5418 \text{ \AA}$ ). Transmission electron microscopy (TEM) was performed with a JEM-3010 electron microscope. High resolution transmission electron microscopy (HRTEM) was performed with a TECNAI F20 electron microscope. Scanning transmission electron microscopy (STEM) was performed with a JEM-2010 electron microscope. The infrared (IR) spectrum was recorded on an IFS-66V FTIR spectrometer.

## 3. RESULTS AND DISCUSSION

The LBZA nanobelts (NBs) were prepared by simply adding water in ZnO ethanol colloids. ZnO ethanol colloids were prepared by a sol-gel method proposed by Spanhel and Anderson, with some modifications.<sup>32,33</sup> It has been well-known that in the structure of LBZA, the zinc hydroxide layers consist of octahedral zinc and tetrahedral zinc.<sup>34</sup> The layer structure can be viewed as edge-sharing octahedra, whereas one-quarter of the octahedral zinc sites are vacant and two tetrahedral zinc locate above and below each octahedral vacant site. Comparing with the brucite-type layers, the continuity of the edge-sharing octahedral layer is broken at the tetrahedral sites. The XRD pattern (Fig. 1(a)) of the precipitates confirmed the formation of LBZA phase, which have been reported by Song et al.<sup>35</sup> The well-known peak at  $2\theta = 6.62^\circ$  suggested an interlayer *d*-spacing of 1.33 nm corresponding to the 001(I) diffraction of the bilamellar phase. The peak at  $2\theta = 13.32^\circ$  and  $20.04^\circ$  could be assigned to its second- and third-order reflection, respectively. Another interlayer distance was found to be 2.03 nm, as determined by the first peak at  $2\theta = 4.36^\circ$ , due to the 001(II) diffraction of the bilamellar phase.

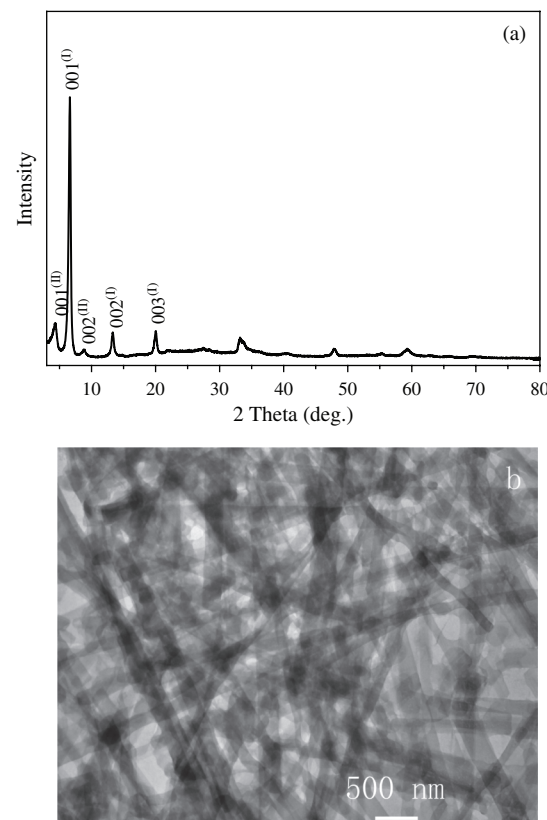


**Figure 1.** (a) XRD pattern and (b) TEM image of the LBZA NBs.

Its corresponding second-order reflection was observed at  $2\theta = 8.94^\circ$ . TEM image showed that the precipitates were consisted of belt-like nanostructures (Fig. 1(b)). Generally, the NBs were 50–200 nm wide and up to 10  $\mu\text{m}$  long. The thickness of NBs was 20–30 nm estimated from some bent NBs. It should be noted that the NBs obtained by this method are much narrower compared with previous work,<sup>35</sup> which should be due to the low preparation temperature and the ethanol-water reaction system.

NWs formed when we dispersed NBs into water and kept for 2 days at room temperature. Abundant NWs with diameter of about 3–5 nm were observed by TEM and dark-field STEM images (Figs. 2(a), (b), and (d)). The NBs were also observed (Fig. 2(a)). We could find some NWs had the same boot due to the inadequate splitting of the NBs (Fig. 2(a)) and some were still connected with plate-like structures (Fig. 2(b)). It was suggested that these NWs were derived from the NBs based on TEM observations. The HRTEM images of NWs are shown in Figure 2(c). We could observe the spacing of 0.281 and 0.261 nm, corresponding to the (100) and (002) planes of hexagonal ZnO, respectively. XRD pattern of the products obtained after keeping the LBZA NBs in water for 2 days is shown in Figure 2(e). The diffraction peaks could be indexed as ZnO and LBZA.

Our investigation revealed that the morphology changed with the incubating time when keeping the NBs in water.

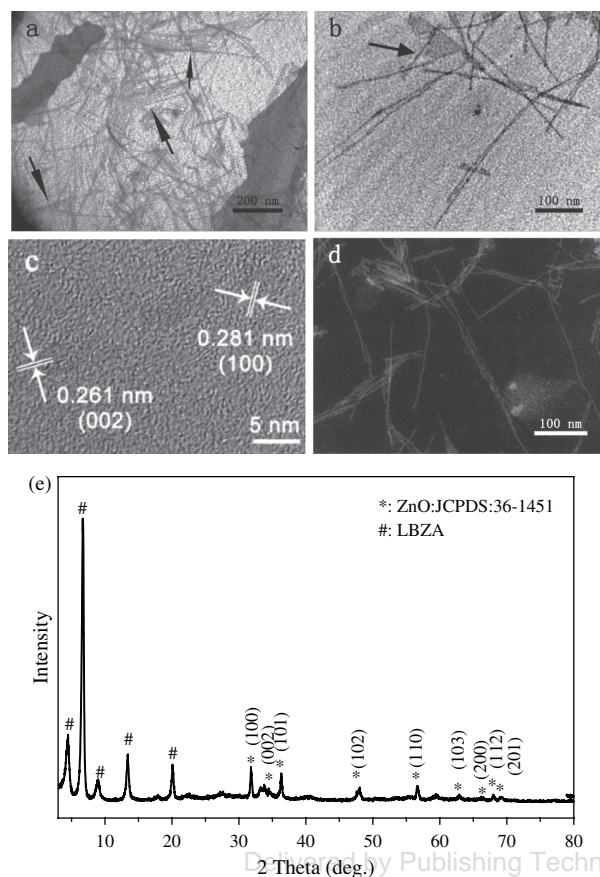


**Figure 2.** (a) and (b) TEM images, (c) HRTEM image, (d) dark-field STEM image and (e) XRD pattern of the products after keeping the LBZA NBs in water for 2 days.

TEM images and XRD patterns of representative samples are shown in Figures 3 and 4. When keeping the NBs in water for 1 day, some irregular sheets and small amount of NWs were obtained (Fig. 3(a)). Long and thin NWs were obtained after an incubating time of 2 day (Fig. 3(b)). When the incubating time was increased to 4 day, nanorods (NRs) formed besides NWs (Fig. 3(c)). However, all NBs were transformed into NWs and NRs after incubating for 6 day (Fig. 3(d)). We found that, with the extension of the incubating time, the peaks of the LBZA gradually disappeared and that of ZnO gradually increased (Fig. 4).

The IR spectrum of the NWs was obviously different from that of the NBs (Fig. 5). The two bands appearing at  $1576\text{ cm}^{-1}$  and  $1402\text{ cm}^{-1}$  of the NBs were assigned to the antisymmetric  $\text{COO}^-$  stretching vibration ( $\nu_a(\text{COO}^-)$ ) and the symmetric  $\text{COO}^-$  stretching vibration ( $\nu_s(\text{COO}^-)$ ) modes, respectively (Fig. 5(b)).<sup>36-39</sup> The difference in the wave numbers ( $\Delta\nu_{a-s} = \nu_a(\text{COO}^-) - \nu_s(\text{COO}^-)$ ) was calculated as  $174\text{ cm}^{-1}$ , which indicates that the coordination type of the acetate groups to zinc cations is a monodentate-type.<sup>38, 40, 41</sup> For NWs, the two bands shifted to  $1508\text{ cm}^{-1}$  and  $1390\text{ cm}^{-1}$ , respectively (Fig. 5(a)). The coordination type was determined as bidentate coordination type based on the value of the  $\Delta\nu_{a-s}$  ( $\Delta\nu_{a-s} = 108\text{ cm}^{-1}$ ). The above data implied that acetates presented in the NWs had different chemical environment compared with that in the NBs. It was possible that the acetates might be present on the surface of NWs. A broad absorption band between  $3750\text{ cm}^{-1}$  and  $3100\text{ cm}^{-1}$  was observed due to the stretching vibration modes of the hydroxyl group and water. At a lower wavenumber range, the IR spectrum of

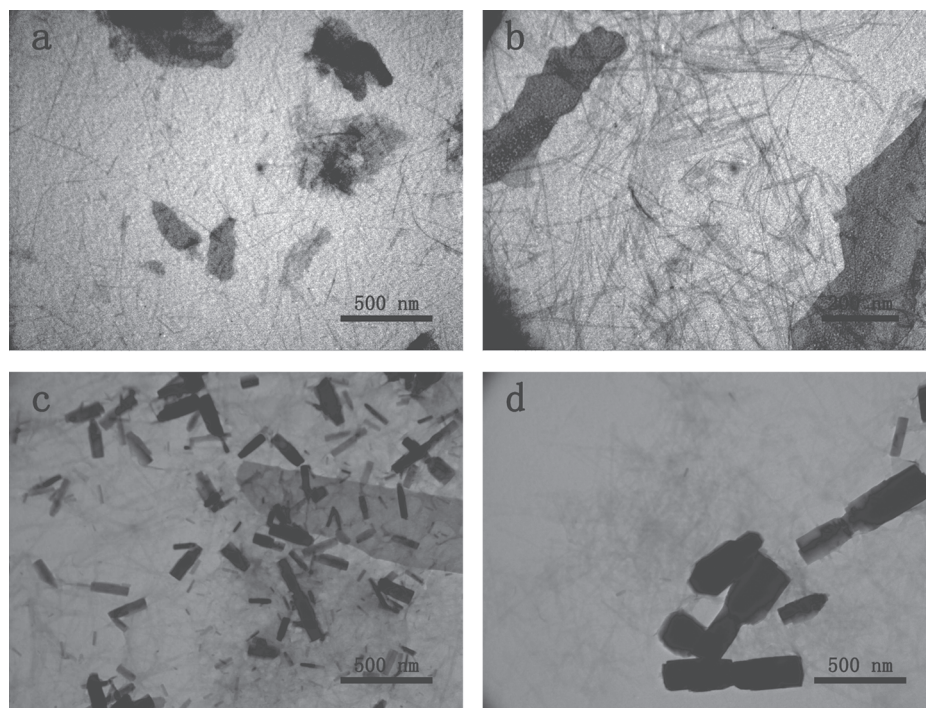


**Figure 3.** TEM images of the products obtained after keeping the LBZA nanobelts in water for (a) 1, (b) 2, (c) 4, and (d) 6 days.

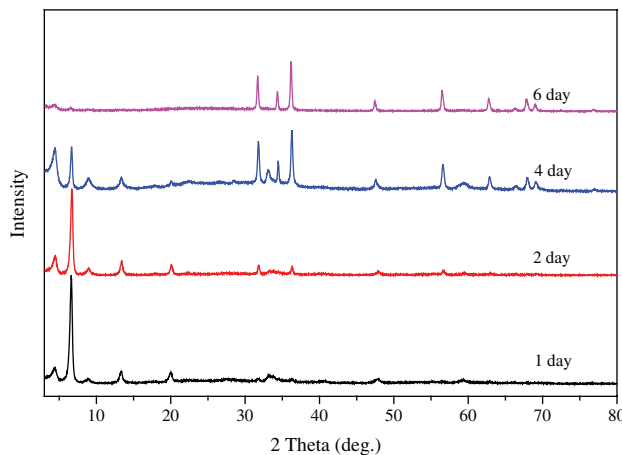


**Figure 4.** XRD patterns of the products obtained after keeping the LBZA nanobelts in water for 1, 2, 4, and 6 days.

NWs was also significantly different from that of the layered compounds, which implied that the structure of NWs was different from that of NBs. The IR results suggested that acetates partially moved out of the layered compound when the NBs were incubated in water. The absence of acetates in the interlayers would result in the bending of the layers at the edge of the NBs. This would bring stress on the layer. Then, collapse of the layers at edge would happen. NWs would form if this process continued.

The reaction for the formation of ZnO NWs and NBs can be expressed as follows:

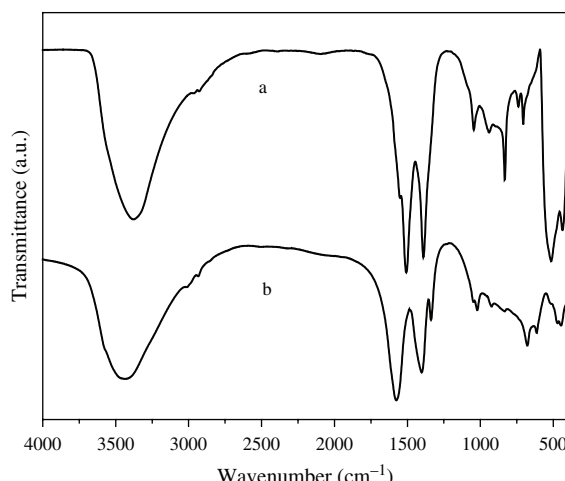
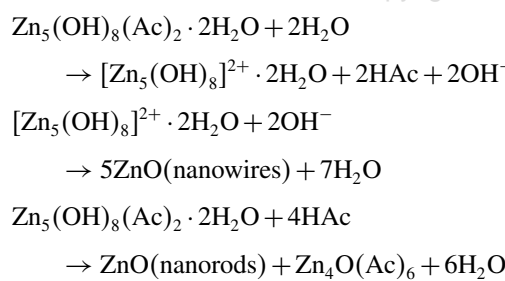
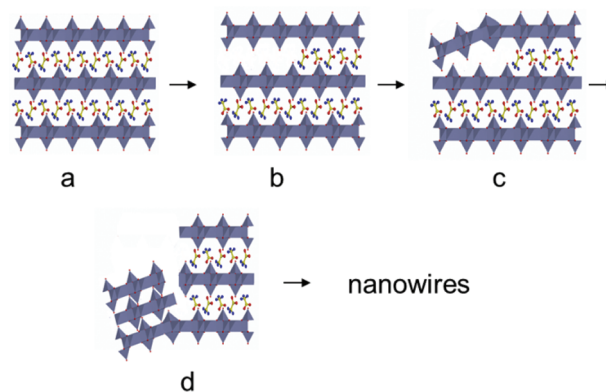


**Figure 5.** IR spectra of (a) ZnO NWs, and (b) LBZA NBs.



**Scheme 1.** The evolution process from LBZA NBs to ZnO NWs. The red, yellow and blue balls represent oxygen, carbon and hydrogen atoms respectively. The zinc hydroxide layers are displayed as polyhedrons based on the coordination environment of zinc atoms.

The formation of ZnO NWs can be schematically described in Scheme 1. The NBs with layered structures (Scheme 1(a)) were incubated in water, the acetate groups left the interlayer (Scheme 1(b)) which was confirmed by IR spectra. The edges of the layers collapsed due to the absence of the acetates in the interlayer (Schemes 1(c) and (d)). Considering the coordination of zinc was different, the collapse would occur at the tetrahedral zinc sites where the continuity of brucite-type layer was broken. We believed that such structure characteristic of LBZA was essential for the observed phenomena. The surface stress on the deformation parts became larger and would drive NBs splitting to positive charged zinc hydroxide NWs. Due to the instability of zinc hydroxide, it was rapidly converted to ZnO. Finally, ZnO NWs were obtained. With the extension of incubating time, acetates in water were gradually increased and reacted with LBZA to generate ZnO NRs (Figs. 3(c) and (d)).

#### 4. CONCLUSIONS

In summary, we prepared ultrathin ZnO NWs by incubating the LBZA NBs in water and discussed the relationship between the morphology of products obtained after incubating and incubating time. The formation process of NWs can be described as the splitting of the layered compound. This result suggests a novel top-down method in preparing ultrathin NWs with layered compound as an intermediate.

**Acknowledgment:** This work was supported by the National Natural Science Foundation of China (No. 21071058).

#### References and Notes

- Y. Xia, P. Yang, Y. Sun, Y. Wu, B. Mayers, B. Gates, Y. Yin, F. Kim, and H. Yan, *Adv. Mater.* 15, 353 (2003).
- K. P. Jayadevan and T. Y. Tseng, *J. Nanosci. Nanotechnol.* 12, 4409 (2012).

3. H. Feng, J. Huang, and J. Li, *Chem. Commun.* 49, 1017 (2013).
4. E. Sutter and P. Sutter, *Nano Lett.* 8, 411 (2008).
5. Y. Tian, M. R. Sakr, J. M. Kinder, D. Liang, M. J. MacDonald, R. L. J. Qiu, H.-J. Gao, and X. P. A. Gao, *Nano Lett.* 12, 6492 (2012).
6. S. H. Kim, A. Umar, S. W. Hwang, S. A. Al-Sayari, M. Abaker, and A. Al-Hajry, *J. Nanosci. Nanotechnol.* 11, 5102 (2011).
7. N. K. Park, S. Y. Lee, and T. J. Lee, *J. Nanosci. Nanotechnol.* 11, 614 (2011).
8. H. Shi, L. Qi, J. Ma, and N. Wu, *Adv. Funct. Mater.* 15, 442 (2005).
9. W. Han, S. Fan, Q. Li, and Y. Hu, *Science* 277, 1287 (1997).
10. J. Lin, Y. Huang, J. Zhang, X. Ding, S. Qi, and C. Tang, *Mater. Lett.* 61, 1596 (2007).
11. Z. Tang, N. A. Kotov, and M. Giersig, *Science* 297, 237 (2002).
12. M. V. Walter, N. Cheval, O. Liszka, M. Malkoch, and A. Fahmi, *Langmuir* 28, 5947 (2012).
13. H. D. Tong, S. Chen, W. G. van der Wiel, E. T. Carlen, and A. van den Berg, *Nano Lett.* 9, 1015 (2009).
14. Z. Li, Y. Chen, X. Li, T. I. Kamins, K. Nauka, and R. S. Williams, *Nano Lett.* 4, 245 (2004).
15. I. Ichinose, J. Huang, and Y.-H. Luo, *Nano Lett.* 5, 97 (2004).
16. A. P. Nayak, T.-C. Lin, D. Lam, S. Kaya, and M. S. Islam, *Nanoscience and Nanotechnology Letters* 4, 977 (2012).
17. D. Pradhan, S. K. Mohapatra, S. Tymen, M. Misra, and K. T. Leung, *Materials Express* 1, 59 (2011).
18. S. H. Ko, D. Lee, H. W. Kang, K. H. Nam, J. Y. Yeo, S. J. Hong, C. P. Grigoropoulos, and H. J. Sung, *Nano Lett.* 11, 666 (2011).
19. K. Chen-Hao and W. Jih-Jen, *Nanotechnology* 18, 505706 (2007).
20. S. Xu, C. Xu, Y. Liu, Y. F. Hu, R. Yang, Q. Yang, J.-H. Ryou, H. J. Kim, Z. Lochner, S. Choi, R. Dupuis, and Z. L. Wang, *Adv. Mater.* 22, 4749 (2010).
21. P.-C. Chang, Z. Fan, C.-J. Chien, D. Stichtenoth, C. Ronning, and J. G. Lu, *Appl. Phys. Lett.* 89, 133113 (2006).
22. M. Yin, Y. Gu, I. L. Kuskovsky, T. Andelman, Y. Zhu, G. F. Neumark, and S. O'Brien, *J. Am. Chem. Soc.* 126, 6206 (2004).
23. H. Yin, Q. S. Wang, S. Geburt, S. Milz, B. Ruttens, G. Degutis, J. D'Haen, L. Shan, S. Punniyakoti, M. D'Olieslaeger, P. Wagner, C. Ronning, and H.-G. Boyen, *Nanoscale* 5, 7046 (2013).
24. D. Stichtenoth, C. Ronning, T. Niermann, L. Wischmeier, T. Voss, C. Chung-Jen, C. Pai-Chun, and L. Jia Grace, *Nanotechnology* 18, 435701 (2007).
25. J. Cui, *Mater. Charact.* 64, 43 (2012).
26. R. Zhu, W. Zhang, and R. Yang, *Science of Advanced Materials* 4, 798 (2012).
27. W.-J. Lee, J.-G. Chang, S.-P. Ju, M.-H. Weng, and C.-H. Lee, *Nanoscale Res. Lett.* 6, 1 (2011).
28. J. Wang and Y. Li, *Adv. Mater.* 15, 445 (2003).
29. C. Li, X. Wang, Q. Peng, and Y. Li, *Inorg. Chem.* 44, 6641 (2005).
30. X. Wang and Y. Li, *Inorg. Chem.* 45, 7522 (2006).
31. F. Ye, Y. Peng, G.-Y. Chen, B. Deng, and A.-W. Xu, *J. Phys. Chem. C* 113, 10407 (2009).
32. L. Spanhel and M. A. Anderson, *J. Am. Chem. Soc.* 113, 2826 (1991).
33. M. Yang, G. Pang, J. Li, L. Jiang, D. Liang, and S. Feng, *The Journal of Physical Chemistry C* 111, 17213 (2007).
34. W. Stahlin and H. R. Oswald, *Acta Crystallogr., Sect. B* 26, 860 (1970).
35. R. Q. Song, A. W. Xu, B. Deng, Q. Li, and G. Y. Chen, *Adv. Funct. Mater.* 17, 296 (2007).
36. L. Poul, N. Jouini, and F. Fiévet, *Chem. Mater.* 12, 3123 (2000).
37. K. J. Scott, Y. Zhang, R.-C. Wang, and A. Clearfield, *Chem. Mater.* 7, 1095 (1995).
38. K. Nakamoto, Infrared and Raman Spectra of Inorganic and Coordination Compounds, Wiley, Weinheim, Germany (1986).
39. A. S. Milev, G. S. K. Kannangara, and M. A. Wilson, *Langmuir* 20, 1888 (2004).
40. M. Nara, H. Torii, and M. Tasumi, *The Journal of Physical Chemistry* 100, 19812 (1996).
41. G. B. Deacon and R. J. Phillips, *Coord. Chem. Rev.* 33, 227 (1980).

Received: 8 July 2013. Accepted: 23 August 2013.